South African Journal of Chemical Engineering 33 (2020) 58–66

Contents lists available at ScienceDirect

South African Journal of Chemical Engineering

journal homepage: www.elsevier.com/locate/sajce

Corrosion and mechanical behaviour Of $Al_2o_3.Tio_2$ composites produced by spark plasma sintering

O.P. Oladijo[a,b,*], A.P.I. Popoola[c], M. Booi[c], J. Fayomi[c], L.L. Collieus[a]

[a] Department of Chemical, Materials and Metallurgical Engineering, Botswana International University of Science and Technology, Palapye, Botswana
[b] Department of Mechanical Engineering Science, FEBE, University of Johannesburg, South Africa
[c] Department of Chemical, Metallurgical and Materials Engineering, Tshwane University of Technology, Pretoria, South Africa.

ARTICLE INFO

Keywords:
$Al_2O_3.TiO_2$ composite
Spark plasma sintering (SPS)
Wear
Corrosion

ABSTRACT

$Al_2O_3.TiO_2$ ceramic composites exhibit versatile properties such as high hardness and excellent wear, chemical, thermal and corrosion resistance. As such, they have been used in various applications such as optical and electronic, gas separation, biomedical processes, and support for transition metal catalysts, wear resistant coatings in machinery, textile and printing industries. However, alumina and alumina-based composites often exhibit high brittleness which limits their potential application as a structural material. In this work, TiO_2 and Al_2O_3 powders at varying compositions were produced through spark plasma sintering (SPS) technique to form $Al_2O_3.TiO_2$ composites. This study investigated the mechanical and anti-corrosion performances of $Al_2O_3.TiO_2$ composites produced by SPS. A higher content of TiO_2 (15wt%) resulted in a lower Vickers's hardness, thus counteracting the intrinsic brittleness in Al_2O_3. Wear resistance also improved with an increase in TiO_2 content up to 10wt%. However, at 15wt% TiO_2, wear resistance decreased due to low hardness. In the sintered samples, secondary phase Al_2TiO_5 was detected and its concentration increased with an increase in TiO_2 content. The microstructure was well reinforced and uniformly. The corrosion resistance in 35 g/l of NaCl solution improved with an increase in the TiO_2 content of up to 10wt%. However, at 15wt% TiO_2, corrosion resistance decreased due to the formation of the secondary phase, Al_2TiO_5.

1. Introduction

Alumina and alumina-based composites have desirable properties as a result of the strong covalent and ionic bonds that exist between their constituent atoms. These strong and directional bonds are responsible for their inherent brittleness which limits their potential application as a structural material (Kumar et al., 2018). In the pursuit counteracting the intrinsic brittleness of these composites, various techniques have been carried out in preparing composites with desirable mechanical properties. One such technique that has been generally accepted by researchers is spark plasma sintering (SPS). The “SPS is a type of sintering technique that makes use of a uniaxial force and pulsed direct electrical current under the influence of low atmospheric pressure, to perform high- speed consolidation of the powder” (Suarez et al., 2013) It is considered as a fast sintering technique in which the heating power is not only evenly dispersed over the volume of the powder compact in a macroscopic scale- but also evaporated exactly at the locations in the microscopic scale where energy is required for the sintering process at the contact points of the powder particles. This results in desirable sintering behavior with minimized grain growth and suppressed powder decomposition (Suarez et al., 2013, Shen et al., 2002). Investigations have indicated that SPS is a promising technique for fabricating composites with improved mechanical properties and microstructural homogeneity. The advantages of SPS over conventional sintering techniques include the ability to sinter the material at low sintering temperatures and in short sintering times, allowing for retention of the initial fine structure that leads to favorable properties (Saheb et al., 2015). Furthermore, SPS is a cost-effective process due to the fact that it does not require a pre-compaction step and can be operated for short times compared to other powder metallurgy processes. The use of additives has also been introduced to these composites as a way of counteracting their intrinsic brittleness by reducing the sintering temperature, customizing the microstructure and thereby improving mechanical properties (Zhang et al., 2013). TiO_2 as an additive to alumina has proved to increase mechanical properties such as hardness and fracture toughness (Kiml and Gauckler, 2012, Manshor et al., 2015) as a result $Al_2O_3.TiO_2$ composites are widely used as wear resistant coatings in machinery, printing industries and textile due to their high

* Corresponding.author.
E-mail address: seyiphilip@gmail.com (O.P. Oladijo).

https://doi.org/10.1016/j.sajce.2020.05.001
Received 12 December 2018; Received in revised form 18 March 2020; Accepted 1 May 2020
1026-9185/ © 2020 The Author(s). Published by Elsevier B.V. on behalf of Institution of Chemical Engineers. This is an open access article under the CC BY-NC-ND license (http://creativecommons.org/licenses/BY-NC-ND/4.0/).

hardness, excellent corrosion, and wear, chemical and thermal resistance" (Bian et al., 2012).

Manshor et al. (2015) carried out the sintering of zirconia-toughened alumina ceramic composites and the amounts of TiO_2 were varied from 0wt% to 10wt%. Results indicated that the fracture toughness and hardness increased from 5.93 MPa.m$^{0.5}$ for 0wt% TiO_2 to 6.56 MPa.m$^{0.5}$ for 3wt% TiO_2 and from 1516 HV for 0wt% TiO_2 to 1615.8 HV for 3wt % TiO_2 respectively. Akin et al. (2010) also studied the effect of TiO_2 addition on the properties of SPS $Al_2O_3.ZrO_2$ composites prepared by SPS. The composites were prepared through SPS technique at temperatures 1300°C, 1350°C, and 1460°C for 300 s under a pressure of 40 MPa. Experimental results indicated that fully dense Al_2O_3 composites containing 0 and 5wt% TiO_2 had a relative density of 99% and the Vickers hardness of the composites under a load of 9.8 N decreased from 19.8 ± 0.4 GPa to 17.3 ± 0.3 GPa with an increase in TiO_2 content. Khaskhoussi et al. (2017) investigated the influence of TiO_2 additions on sintering behavior of ZrO_2 and $Al_2O_3.ZrO_2$ for dental applications. Alumina-titania, zirconia-titania, and titania-alumina-zirconia powders were uniaxially pressed and pressureless sintered at 1400°C for 2 hours. Results indicated reduced grain growth of alumina and that the inter-granular porosity was suppressed by the addition of 5wt% and 10wt% of titania. The high reactivity of nano-TiO_2 resulted in the formation of several phases which could have an influence on mechanical properties.

Wahsh et al. (2013) worked on the sintering and technological properties of alumina/ zirconia/ nano-TiO_2 ceramic composites and observed one such phase. The authors indicated that the combination of Al_2O_3 and TiO_2 leads to the formation of Al_2TiO_5 that exhibits high resistance to thermal shock among all other ceramics. However, the presence of Al_2TiO_5, a ceramic with low thermal expansion results in the formation of micro-cracks at the grain boundaries and consequently absorbs the energy of the crack tip thus arresting its propagation (Kiml and Gauckler, 2012). The authors mentioned that the thermal durability of Al_2TiO_5 can be improved by the formation of solid solutions with MgO or Fe_2O_3. Furthermore, the addition of SiO_2, ZrO_2, and $ZrTiO_4$ limits micro-cracks, micro-cracks growth and grain growth. Previous studies have reported on the mechanical properties of $Al_2O_3.TiO_2$ composites fabricated by SPS technique. However, the anti-corrosion performances of the SPS composites have rarely been reported which leaves ample opportunity to study the corrosion properties of these composites. Furthermore, scarce information is available in the literature as to how to counteract the inherent brittleness present in Al_2O_3 and Al_2O_3 composites. Al_2O_3 inherently possesses strong corrosion resistance, this work will therefore investigate the effect of incorporating TiO_2 on the bulk corrosion resistance and the mechanical performance of $Al_2O_3.TiO_2$ composites produced by SPS technique. Six samples of $Al_2O_3.TiO_2$ composites of varying compositions will be fabricated through SPS technique. The effect of the varying compositions on the mechanical and corrosion properties of the sintered samples have been studied and characterization focused on microstructural, corrosion and mechanical behavior of the samples will be made.

2. Experimental materials and methods

2.1. Powder preparation

Commercial alumina (Al_2O_3) nano powder of purity 99.7%, 40 nm particle size and TiO_2 of 99.7% purity, 40 – 50 nm particle size was employed in this work. All the powders were supplied by Hongwu International Group, China. The powders were weighed according to compositions of the samples. Samples 1A and 1B contained 99.5wt% Al_2O_3 and 0.5wt% TiO_2, samples 2A and 2B contained 90wt% Al_2O_3 and 10wt% TiO_2, while samples 3A and 3B contained 85wt% Al_2O_3 and 15wt% TiO_2.

The weighed powders were transferred into plastic containers and mixed in a dry mode using a Tubular Shaker Mixer (model T2F) at a rotating speed of 110 rpm for 10 h to ensure homogeneous mixing. Some steel balls (8 mm diameter) were incorporated into the powder container during the mixing operation at the ball to powder ratio of 2:5 for a better dispersion of the reinforcements in the matrix following the method used by (Ujah et al., 2018).

Table 1
Sample composition and sintering temperature.

Sample	Composition (*wt %*)	Sintering Temperature (°*C*)
1A	0.5 TiO_2, 99.5 Al_2O_3	1350
1B	0.5 TiO_2, 99.5 Al_2O_3	1650
2A	10.0 TiO_2, 90.0 Al_2O_3	1700
2B	10.0 TiO_2, 90.0 Al_2O_3	1650
3A	15.0 TiO_2, 85.0 Al_2O_3	1500
3B	15.0 TiO_2, 85.0 Al_2O_3	1650

2.2. Spark plasma sintering of the samples

The powders were weighed into a graphite die which was used as sample holder and sintered at temperatures of 1350, 1500, 1650 and 1700°C as shown in Table 1, with the heating rate, holding time and sintering pressure held constant at -173.15°C/min, 5 min and 50 MPa, respectively. Each sample was transferred into a mould and thereafter punched on both sides using appropriate dies before being taken to the sintering machine. Graphite sheets were used to shield the powders to ensure easy removal of sintered samples and reduction of temperature gradients across the samples. To obtain pure sinter products, graphite was finally blasted off the sintered samples using a sandblasting machine. This was done to increase the accuracy of densification measurements to be done on each sample using the density meter.

2.3. Density measurements of the spark plasma sintered samples

The densification of the sintered samples was measured using the rule of mixture and Archimedes principle which in involves weighing the polished sample specimen in air and immersed in distilled water, rule of the mixture is a method used to estimate theoretical density of composite materials based on the assumption that a bulk composite property is the percent volume fraction of the matrix.

Using a weigh balance, the samples were weighed 3 times in both air and distilled water and the average masses were used to compute the relative density of the samples. The density of the samples was then determined from the equation;

$$\rho_c = \frac{m_{air}}{m_{air} - m_{water}} \tag{3}$$

Where;

- ρ_C = *Density of the composite*
- m_{air} = *mass in air*
- m_{air} = *mass in water*

2.4. Sample preparation (cutting, mounting, grinding and polishing)

Samples for corrosion and hardness tests and SEM and XRD analysis were cut into 10×10 mm sections and the wear test samples were sectioned into 15×15 mm. Samples were then cold mounted to ease grinding and polishing which removes surface impurities, in order to obtain characterization results representative of the bulk material. Aka Piatto 120 disc, was used for grinding and the second and third stages of polishing were done using Aka-Allegran 9 grit disc coupled with a Diamaxx 9 um mono solution and Aka-Rhaco with a 3 um mono solution. Polishing was done until a smooth, shiny and scratch-free surface was obtained on each sample.

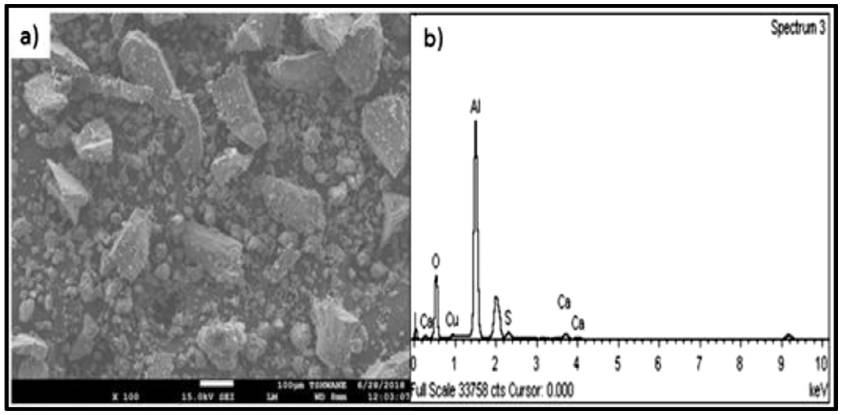

Fig. 1. Shows (a) overall morphology of Al_2O_3 powder and (b) EDS spectrum of the elemental composition of the powder.

2.5. Characterization of powders and sintered samples (SEM, EDS, XRD)

The X-ray diffraction (XRD) machine was used for phase identification analysis of the powders and sintered samples. The analysis was conducted with a Cu-Kα radiation at 40 kV and 20 mA on D8 Discovery. The microstructural analysis, surface topography, morphology, and compositions was conducted and with field-emission scanning electron microscope (FE-SEM, TESCAN, Brno, Czech Republic) equipped with energy dispersive X-ray spectroscopy (EDS, Oxford Instruments, Oxfordshire, UK), the microstructure of the sintered samples was analysed.

2.6. Mechanical properties (Vickers micro-hardness and abrasive wear tests)

A testing load of 1000 kN was used on the samples for the Vickers micro-hardness test and the indents were observed by microscope. Each sample was dented three times and the average was computed using the following equation;

$$HV = 1.854 \cdot \frac{F}{\left(\frac{D1 + D2}{2}\right)^2} \tag{4}$$

The RTEC 2441 USA universal tribometer was used to measure the abrasive wear rate of the sintered samples. Wear tests for all samples were conducted under a load of 150 N with a sliding distance of 5 mm at a speed of 3 mm/s. The wear rate was then calculated from the height loss technique and expressed in terms of the wear volume loss per unit sliding distance as shown in the equation;

$$K = \frac{V}{F \cdot D_{slidIng}} \tag{5}$$

Where;

- $K = Wear\ Rate$
- $V = (Initial\ mass - Final\ mass)/(Actual\ density\ of\ composite)$
- $D_{sliding} = Sliding\ Distance$
- $F = Applied\ Force$
- $D1\ and\ D2 = Diagonal\ lengths\ of\ the\ dent$

2.7. Electrochemical corrosion test in 35 g/L NaCl solution

The corrosion behavior of the composite material was assessed using an Autolab Potentiostat (PGSTAT302N) controlled by the NOVA software version (1.9). Linear polarisation experiment was run at the current range of 100 mA and 100 μA, open circuit polarisation (OCP) of 120 s, start and stop potentials of −1.5 V and +1.5 V, with a scan rate of 0.01 V/s. The electrodes consists of the reference electrode of Ag/AgCl in KCl solution, a counter electrode of platinum and a working electrode where the test samples were connected. The electrolytes included 35 g/L of NaCl solution (Ujah et al., 2018). The electrolyte solution was prepared using distilled water in a Merrian beaker. Tafel extrapolation was used to obtain corrosion rate, corrosion potential, current density, and the polarization potential.

The equipment uses three electrodes to investigate the reaction mechanisms of the working metals or alloy which are: the reference electrode, the counter electrode and the working electrode which hold the test sample. The electrodes are connected to an electronic potentiostat and placed inside an electrolyte usually of different medium (acidic, Alkaline, saline). An electric potential is passed across the set-up while the potentiostat measures the energy difference between the working electrode and the reference electrode.

3. Results and Discussion

3.1. Characterization of powders

3.1.1. SEM/EDS analysis of as-received powders

The morphology of the as-received Al_2O_3 powder is shown in Fig. 1 (a) and the EDS results in 1 (b). The powder revealed polyhedral, irregular and angular shapes with a particle size distribution ranged at 40-50 nm. The presence of Ca, Cu and S are attribute to minor impurities in the powder.

Analysis of the as-received TiO_2 powder as shown in Fig. 2 (a) and (b) revealed finely sized particles and traces of Al, S and other minor elements, respectively.

3.1.2. XRD of as-received powders

XRD results of the pure unmixed powders; Al_2O_3 and TiO_2 as shown in Fig. 3, only confirmed the presence of Al_2O_3 and rutile as expected, which agrees with literature.

Upon mixing, three samples; 1A, 2A and 3A of respective compositions; 99.5wt% Al_2O_3 and 0.5wt% TiO_2, 90wt% Al_2O_3 and 10wt% TiO_2 and 85wt% Al_2O_3 and 15wt% TiO_2, were produced. The XRD pattern of the three samples as seen in Fig. 4, revealed peaks that only identified Al_2O_3 and rutile. Al_2O_3, recorded the highest peaks, implying that it was the base material on all the samples.

3.2. SEM/EDS analysis of sintered samples

Fig. 5 shows the SEM and EDS analysis of the sintered samples. EDS revealed dark grey grains of Al_2O_3 and light grey-whitish grains of TiO_2, Al_2O_3/TiO_2 or Al_2TiO_5. The grains were of a uniform size and morphology and they were uniformly distributed throughout the matrix. Results of samples 3A and 3B shown in Fig. 5 e and f, respectively, showed that TiO_2 completely reacted with Al_2O_3 to form secondary phase Al_2TiO_5. According to Yang et al. (Ujah et al., 2018) “for the

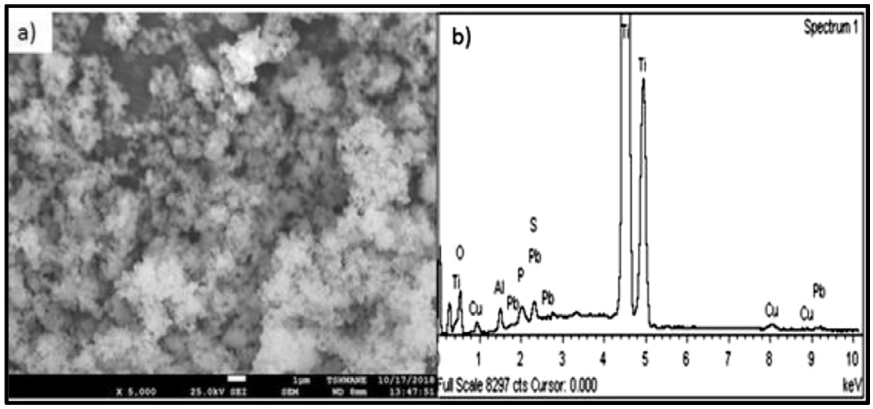

Fig. 2. Shows (a) overall morphology of TiO_2 powder and (b) EDS spectrum of the elemental composition of the powder.

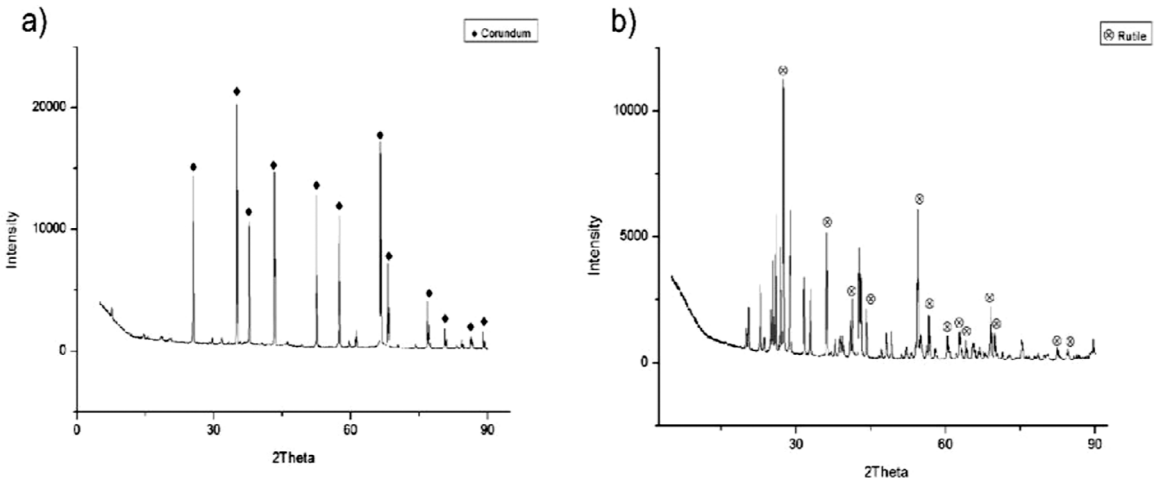

Fig.3. XRD analysis of a) Al_2O_3 and b) TiO_2 powders.

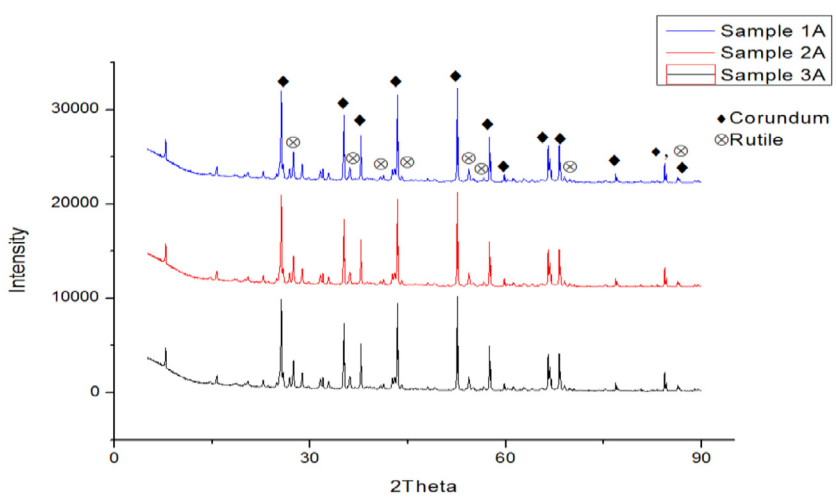

Fig. 4. XRD analysis of the mixed (Al_2O_3 .TiO_2) powders.

alumina-titania system, when the amount of titania is above the solution limit (lower than 0.5wt% in the temperature range 25 - 1700°C) within alumina, the excess titania coexists with alumina below 1280°C. Above this temperature, in an oxidizing atmosphere, the solid state reaction below is possible;

$$\alpha - Al_2O_3 + TiO_2 \rightarrow Al_2TiO_5$$

3.3. XRD analysis of sintered samples

Fig. 6 shows the XRD pattern of the sintered samples. It is evident that the formation and increase of the secondary phase Al_2TiO_5 is dependent on the increase of TiO_2. At high contents of TiO_2 (15wt %), only Al_2O_3 and Al_2TiO_5 phases were present, which implies that TiO_2 completely reacted with Al_2O_3 to form the secondary phase, Al_2TiO_5.

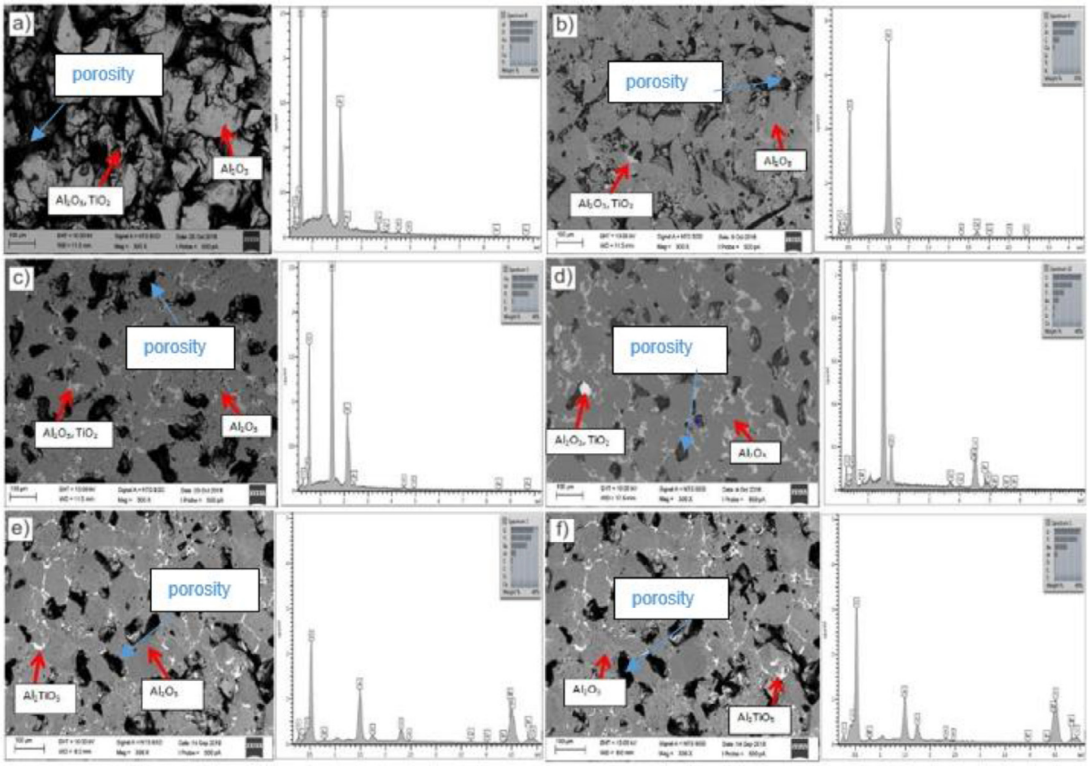

Fig. 5. SEM/EDS micrographs of samples; a) 1A sintered at 1350°C, b) 1B at 1650°C, c) 2A at 1700°C, d) 2B at 1650°C, e) 3A at 1500°C and f) 3B at 1650°C.

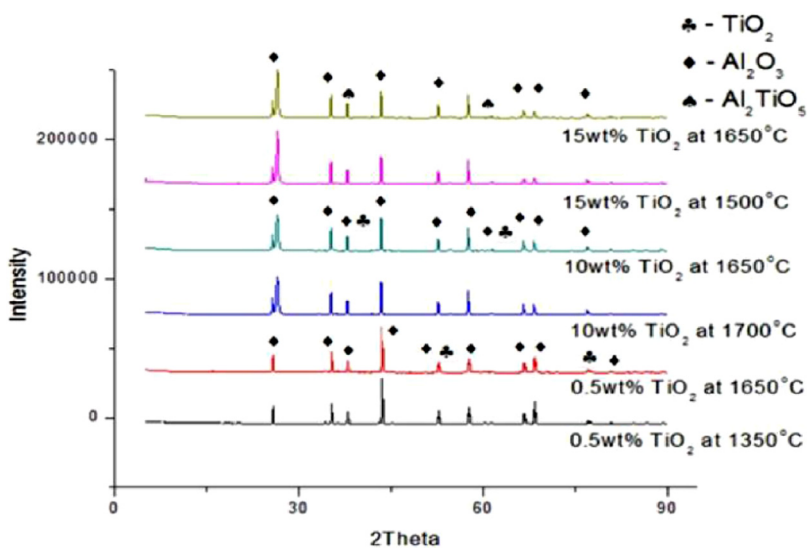

Fig. 6. XRD pattern of the sintered samples.

Table 2
Results of the sintered samples.

Sample	Densification (%)	Vickers Hardness (MPa)	Abrasive wear rate (m^2/N)	Average coefficient of friction
1A	77	12852	0.031	0.18
1B	89	10895	0.035	0.13
2A	89	12534	0.034	0.10
2B	87	13622	0.023	0.11
3A	90	2959	0.011	0.11
3B	88	2339	0.013	0.10

3.4. Densification results

Samples 1A and 1B which had the same composition of 0.5wt% TiO_2 and 99.5wt% Al_2O_3 and different sintering temperatures of 1350°C and 1650°C respectively, as seen in Table 2, had different densification%, with that of sample 1B being higher than that of 1A. This proves that the densification% for these samples increases with increasing sintering temperature.

Samples 2A and 2B, of composition 10wt% TiO_2 and 90wt% Al_2O_3, were sintered at 1700°C and 1650°C respectively. The same trend in samples 1A and 1B of the densification% with sintering temperature was observed in Fig. 7. An exception between samples 3A and 3B was evident with the densification% of 3A sintered at 1500°C being higher

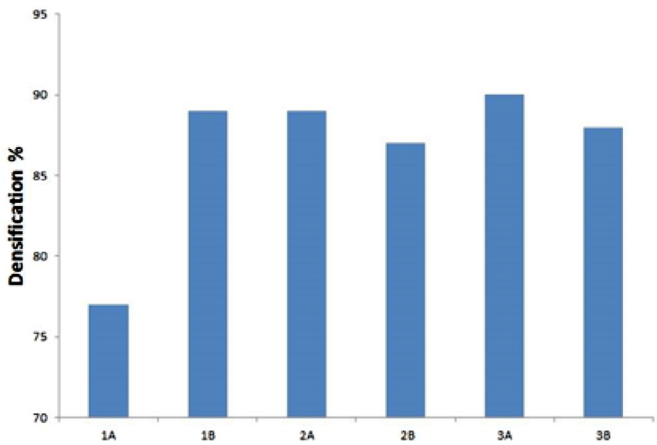

Fig. 7. Variation of the Densification Results.

Table 3
Electrochemical corrosion results.

Sample	Ecorr, Obs (V)	jcorr (A/cm^2)	Corrosion rate (mm/year)	Polarization resistance (Ω)
1A	-0.39838	1.63E-10	1.73E-06	4.25E + 08
1B	-0.38651	1.52E-06	0.021081	169120
2A	-0.32305	1.65E-06	0.017506	43142
2B	-0.39136	3.49E-07	0.0040243	223330
3A	-0.42928	2.58E-06	0.024219	12433
3B	-0.37136	1.62E-06	0.012468	12120

than that of 3B sintered at 1650°C. However, it was noted that the densification% of all the samples was quite low, implying high porosity within the sintered composites. According to Yang, (2009), porosity may arise from; (1) formation of gases in the sintering process and their subsequent expansion, entrapment or escape, (2) shrinkage associated with the reaction that takes place during the sintering process (i.e. products that have a higher specific volume than the starting materials or (3) residual initial porosity of the powder due to partial sintering. When comparing samples 1B (0.5wt% TiO_2 & 99.5wt% Al_2O_3) and 2B (10wt% TiO_2 & 90wt% Al_2O_3) which were sintered at the same temperature of 1650°C, the densification% decreased with increasing TiO_2. This may be attributed to the possible formation of a secondary Al_2TiO_5 phase which is hard to sinter and has a lower density of 3.7 g/cm^3 relative to those of alumina, 3.95 g/cm^3 and titania, 4.23 g/cm^3 (Yang, 2009). High-temperature sintering (1650°C) of higher TiO_2 content failed to improve the densification% due to the presence of Al_2TiO_5 phase which is hard to sinter (Yang, 2009).

3.5. Vickers micro-hardness test

Comparing samples 1B, 2B and 3B, all sintered at 1650°C, hardness increased with an increase in reinforcement from samples 1A to 1B. This increase may be attributed to the presence of rutile phases that are dispersed in the alumina matrix. Small quantities of TiO_2 have been proved to act as a strong reinforcing Nano material in the developed composite and the formation of the Al_2TiO_5 secondary phase was observed to increase and improve mechanical properties (Zhan and Li, 2015).

However, a sharp decrease in hardness from sample 2B to sample 3B was observed. According to Verma and Manoj (2017), this is due to the presence of Al_2TiO_5 phase which thermally dissociates under high temperature, producing micro-cracks that rapidly decrease hardness. Moreover, weak covalent and ionic bonds that exist between the constituent atoms contribute to this abrupt decrease (Kiml and Gauckler, 2012). Previous reports have shown that alumina exhibits intrinsic brittleness due to its high hardness. This brittle nature can be countered by increasing the TiO_2 contents at higher intense temperature in the mixture. However, the decrease in the hardness as a result of TiO_2 inclusion at higher sintered temperature was affirmed by the increase in the porosity level and this was evident in the SEM microstructure.

3.6. Abrasive wear test

A universal tribometer was used to characterize the wear behavior of the sintered samples. Comparing samples of the same composition but different sintering temperatures on Fig. 9a, the wear rate proved to be higher for samples sintered at higher temperatures. This is expected, as samples sintered at lower temperatures relative to their counterparts of the same composition exhibited increased hardness. Therefore, it can be concluded that wear resistance decreases at high sintering temperatures.

Samples 1B, 2B and 3B of different chemical compositions but same sintering temperature of 1650°C shown in Fig. 9b, showed a decrease in wear rate with increasing TiO_2 content. Therefore, sample 3B showed the lowest wear rate and thus better wear resistance.

Fig. 10 shows the wear tracks of the sintered samples which were captured using optical microscopy. To understand the wear behavior, the wear scars were studied. Similar scars were observed on all the sintered samples, although the extent of damage was different. This is due to their differences in composition and the residual stress effect, which was not considered in this work.

3.7. Electrochemical corrosion test in 35 g/l of NaCl solution

The corrosion results obtained from a tafel extrapolation plot and were plotted in Fig. 20 below and summarized in Table 3. Comparing samples 1A and 1B which had the same composition but different

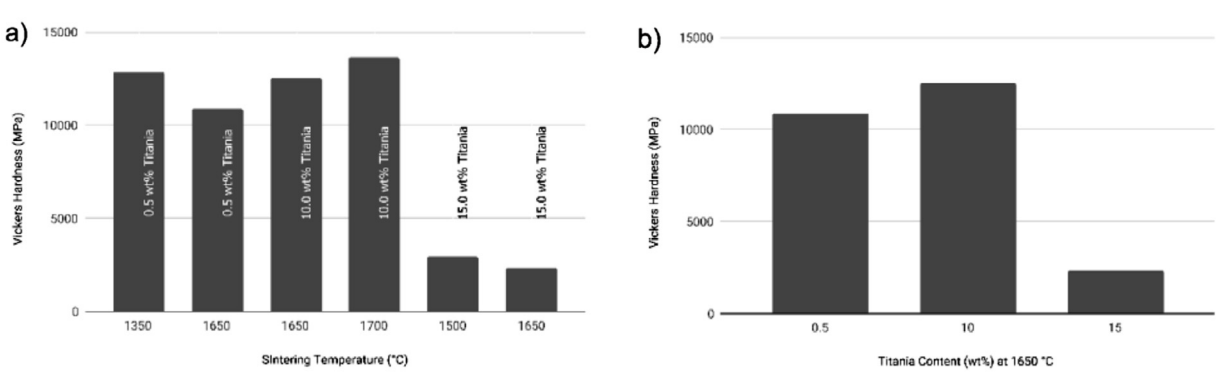

Fig. 8. Vickers micro-hardness of the sintered samples against a) sintering temperature and b) titania content at 1650°C sintering temperature.

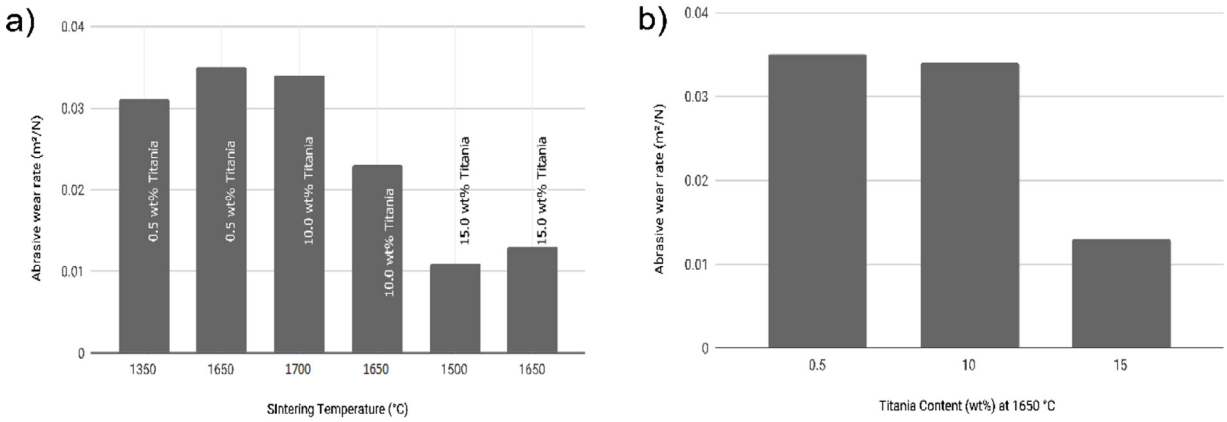

Fig.9. Abrasive wear of the sintered samples against a) sintering temperature and b) titania content at 1650°C sintering temperature.

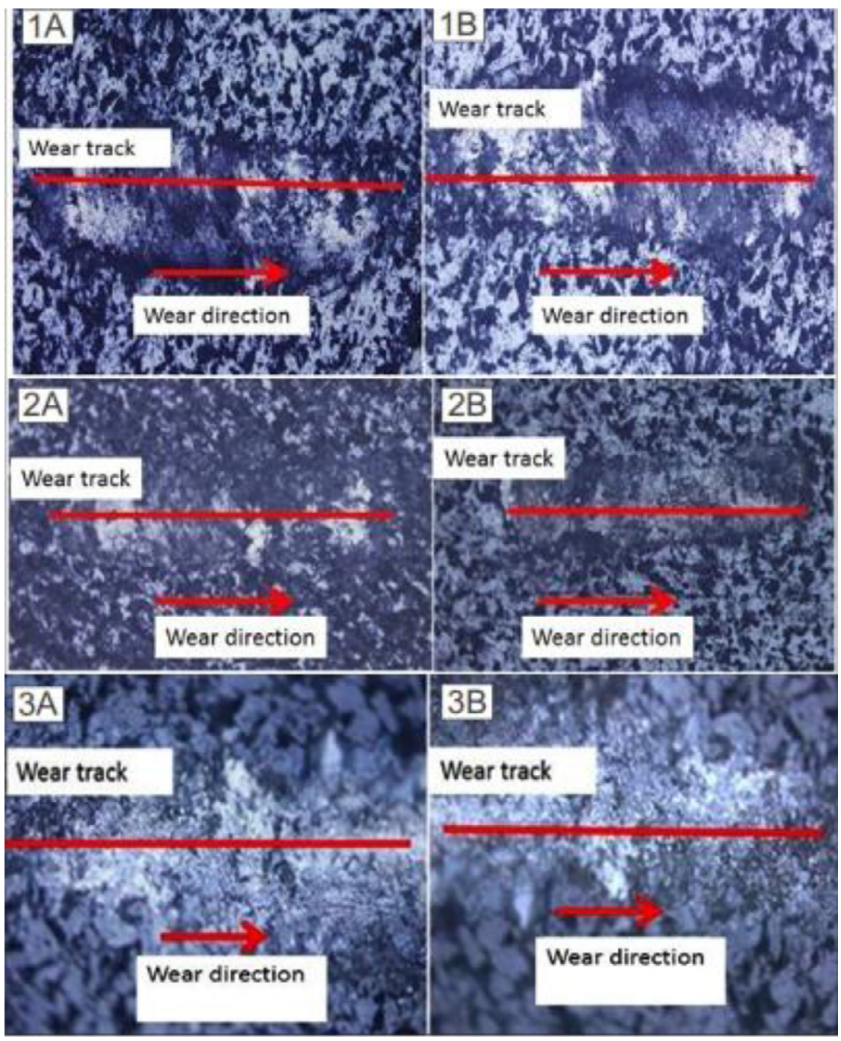

Fig. 10. Micrograph showing wear tracks of the samples at 5x magnification.

sintering temperatures of 1350°C and 1650°C, respectively, showed that 1A had a better corrosion resistance than sample 1B. The corrosion rate of sample 1A was 1.73E-06 mm/year and its polarization resistance was 4.25E + 08 Ω, while sample 1B had a corrosion rate of 0.021081 mm/year and polarization resistance of 169120 Ω.

For samples 2A and 2B sintered at 1700°C and 1650°C, respectively, sample 2B showed more resistance to corrosion than sample 2A. The corrosion rate and polarization resistance of sample 2A was 0.017506 mm/year and 43142 Ω, respectively, while that of sample 2B was 0.0040243 and 223330 Ω respectively. Samples 3A and 3B, sintered at 1700 and 1650°C, respectively, had corrosion rates of 0.024219 and 0.012468 mm/year with polarization resistances at 12433 and 12120 Ω, respectively. At high sintering temperatures the composite seems to be more susceptible to salt-water corrosion than at lower temperatures of the same composition. Samples 1A, 2B and 3B are therefore advised for applications in saline environments.

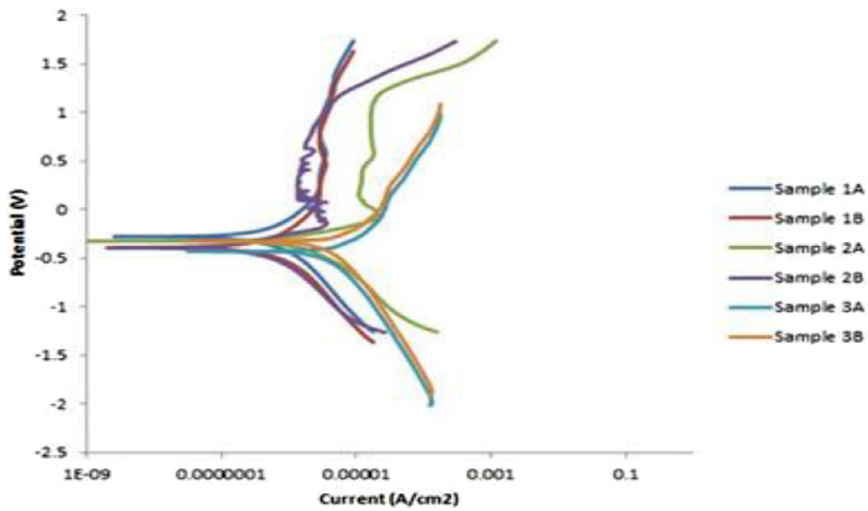

Fig. 11. Linear polarization curves of the sintered samples in 35 g/L of NaCl solution.

Sample 1B, 2B, and 3B were sintered at the same temperature of 1650°C and amongst the three samples, 2B was more resistant to corrosion. At higher reinforcement material (10wt% TiO_2), the corrosion rate of the composite was low while the polarization resistance was high and vice-versa for lower reinforcement material of 0.5wt% TiO_2. However, at 15wt% TiO_2, the corrosion rate increased thereby resulting in a lower corrosion resistance. This may be due to the formation of Al_2TiO_5 phase which is highly susceptible to thermal dissociation especially at higher temperature ranges of 1000°C and above. Therefore, the presence of such a phase in the sintered composite will act as corrosion initiation sites thereby decreasing alumina's inherent good corrosion resistance. Sample 2B is therefore the preferable choice for applications in a saline environment.

4. Conclusion

The anti-corrosion and mechanical performances of $Al_2O_3.TiO_2$ composites produced by spark plasma sintering were investigated. The following conclusions were drawn from the study that was conducted:

- The spark plasma sintering of $Al_2O_3.TiO_2$ composites were carried out successfully.
- Vicker's hardness increased with increase in TiO_2 content up to 10wt % TiO_2. However, a sharp decrease in hardness was noted for 15wt % TiO_2. As such, higher content of TiO_2 resulted in lower hardness, thus counteracting the intrinsic brittleness in Al_2O_3.
- Wear resistance increased with an increase in TiO_2 content up to 10wt% TiO_2. However, wear resistance decreased for 15wt% TiO_2 sample due to its low hardness.
- A secondary phase Al_2TiO_5 was detected in samples with 15wt% TiO_2 sintered at 1500 and 1650°C.
- The microstructures of the sintered samples were well reinforced and uniformly distributed.
- Corrosion resistance in 35 g/L of NaCl solution increased with an increase in TiO_2 content up to 10wt%. However, it decreased at 15wt% TiO_2 due to the formation Al_2TiO_5 phase which was detrimental to alumina's natural tendency to resist corrosion.

Fig. 8, Fig. 11

CRediT authorship contribution statement

O.P. Oladijo: Conceptualization, Methodology, Supervision, Project administration. **A.P.I. Popoola:** Resources, Writing - review & editing, Funding acquisition. **M. Booi:** Writing - original draft, Formal analysis, Investigation, Visualization. **J. Fayomi:** Methodology, Resources, Validation, Writing - review & editing, Project administration, Supervision. **L.L. Collieus:** Visualization, Writing - review & editing.

Declaration of Competing Interest

○ All authors have participated in the analysis and interpretation of the data; drafting and revising of the article. All authors made an approval of the final version.

○This manuscript has not been submitted to, nor is under review at, another journal or other publishing venue.

○The following authors have affiliations with organizations with direct or indirect financial interest in the subject matter discussed in the manuscript:

Acknowledgments

The authors would like to appreciate the financial support of the NRF, South Africa. The equipment support at the Botswana International University of Science and Technology, Palapye is highly appreciated.

References

Akin, I., Yilmaz, O., Ormanci, F., Sahin, F., Yucel, F., Goller, G., 2010. Effect of TiO_2 addition on the properties of $Al_2O_3.ZrO_2$ composites prepared by spark plasma sintering. Bioceramics Dev. Appl. 1, 3.

Bian, H., Yang, Y., Wang, Y., Wei, T., 2012. Preparation of nanostructured alumina- titania composite powders by spray drying, heat treatment and plasma treatment. Powder Technol. 219, 257–263.

Khaskhoussi, A., Calabrese, L., Bouaziz, J., Edoardo, P., 2017. Effect of TiO_2 addition on microstructure of zirconia/ alumina sintered ceramics. Ceramics Int. 43, 10392–10402.

Kiml, I., Gauckler, G, 2012. "Formation, decomposition and thermal stability of Al_2TiO_5 ceramics. J. Ceramic Sci. Technol. 3, 49–60.

Kumar, R., Chaubey, A.K., Maity, T., Khasanov, O., 2018. "Mechanical and tribological properties of Al_2O_3.TiC composite fabricated by spark plasma sintering process with metallic (Ni, Nb) binders. Metals 8, 50.

Manshor, H., Aris, S.M., Azhar, Z.A., Ahmad, Z.A., Abdullah, E.C, 2015. Effects of TiO_2 addition on the phase, mechanical properties, and microstructure of zirconia-toughened alumina ceramic composite. Ceramics Int. 41, 3961–3967.

Saheb, N., Khan, R.S., Hakeem, A.S., 2015. "Effect of processing on mechanically alloyed and spark plasma sintered $Al.Al_2O_3$ nanocomposites. J. Nanomater. 2015, 1–13.

SHEN, Z., JOHNSSO, M., ZHAO, Z., NYGREN, M., 2002. Spark plasma sintering of alumina. J. Am. Soc. 85, 1921–1927.

SUAREZ, M., FERNÁNDEZ, A., MENÉNDEZ, J.L., TORRECILLAS, R., KESSEL, H.U., HENNICKE, J., KIRCHNER, R., KESSEL, T., 2013. Challenges and opportunities for spark plasma sintering: a key technology for a new generation of materials. Intech.

UJAH, C.O., POPOOLA, A.P.I., POPOOLA, O.M., AIGBODION, V.S., 2018. "Electrical conductivity, mechanical strength and corrosion characteristics of spark plasma sintered Al.Nb nanocomposite. Int. J. Adv. Manuf. Technol. https://doi.org/10.1007/

s00170-018-3128-x.
VERMA, V., MANOJ, K.B., 2017. Synthesis, microstructure and mechanical properties of Al2O3/ZrO2/CeO2 composites with addition of nickel and titania processed by conventional sintering. Mater. Today: Proc. 4 (2), 3062–3071.
WAHSH, M.M.S., KHATTAB, R.M., ZAWRAH, M.F., 2013. Sintering and technological properties of alumina/ zirconia/ nano-TiO_2 ceramic composites. Mater. Res. Bull. 48, 1411–1414.
YANG, Y., 2009. "In situ porous alumina/ aluminium titanate ceramic composite prepared by spark plasma sintering from nanostructured powders. Scripta Materialia 60, 578–581.
ZHAN, FAN, LI, GLIANG-FENG, 2015. Effect of micro-alumina content on mechanical properties of Al_2O_3/3Y-TZP composites. Ceramics Int. 41, 12417–12425.
ZHANG, J., TU, R., GOTO, T., 2013. "Spark plasma sintering of Al_2O_3.Ni nanocomposites using Ni nanoparticles produced by rotary chemical vapour deposition. J. Eur. Ceramic Soc. 34, 435–441.